

Unsources Random Access with a Massive MIMO Receiver Using Multiple Stages of Orthogonal Pilots

Mohammad Javad Ahmadi and Tolga M. Duman
Department of Electrical and Electronics Engineering
Bilkent University, Ankara, Turkey
{ahmadi, duman}@ee.bilkent.edu.tr

Abstract—We study the problem of unsourced random access (URA) over Rayleigh block-fading channels with a receiver equipped with multiple antennas. We employ multiple stages of orthogonal pilots, each of which is randomly picked from a codebook. In the proposed scheme, each user encodes its message using a polar code and appends it to the selected pilot sequences to construct its transmitted signal. Accordingly, the received signal consists of superposition of the users' signals each composed of multiple orthogonal pilot parts and a polar coded part. We use an iterative approach for decoding the transmitted messages along with a suitable successive interference cancellation scheme. Performance of the proposed scheme is illustrated via extensive set of simulation results which show that it significantly outperforms the existing approaches for URA over multiple-input multiple-output fading channels.

I. INTRODUCTION

Massive multiple-input multiple-output (MIMO) systems achieve high spectral efficiencies, high energy efficiencies, high data rates, and spatial multiplexing gains by creating a massive number of spatial degrees of freedom (DoF) [1]. The original applications of massive MIMO have been in broadband communications [1]–[4]; however, more recently, it has also been proposed for Internet-of-Things (IoT) networks in which a very large number of devices sporadically transmit data to a common access point. The so-called *unsourced random access* (URA), which is introduced by Polyanskiy in [5], is a paradigm suitable for many applications in IoT networks, where the base station (BS) only cares about the transmitted messages, and the identity of the users is not of concern.

In URA, all the active users share the same codebook for their transmission, and the per-user probability of error (PUPE) is adopted as the performance criterion. Many low-complexity coding schemes are devised for URA over a Gaussian multiple-access channel (GMAC) including T-fold slotted ALOHA (SA) [6]–[9], sparse codes [10]–[14], and random spreading [15]–[17]. However, GMAC is not a fully realistic channel model for wireless communications. Therefore, in [18]–[21], the synchronous Rayleigh quasi-static fading MAC is investigated, and the asynchronous set-up is considered in [22], [23]. Recently, several studies have also investigated Rayleigh block-fading channels in a massive MIMO setting. In [24], a covariance-based activity detection (AD) algorithm is used to detect the active messages, while [25] employs rank-1 tensors constructed from Grassmannian sub-constellations.

Furthermore, a pilot-based scheme is introduced in [26] where non-orthogonal pilots are employed for detection and channel estimation, and a polar list decoder is used for decoding messages.

The coherence blocklength is defined as the period over which the channel coefficients stay constant. As discussed in [24], depending on the environment, the coherence blocklength of wireless systems in the URA setting may vary in the range of $100 \leq T_c \leq 2 \times 10^4$, where T_c is measured in terms of the number of transmitted symbols. Although the AD algorithm in [24] performs well in fast fading (e.g., when $T_c \leq 320$), it is not implementable with larger blocklengths due to run-time complexity scaling with T_c^2 . In contrast, the schemes in [25], [26] work well only in the large-blocklength regimes (e.g., for $T_c = 3200$); that is, in a slow fading environment where large blocklengths can be employed, their decoding performance is better than that of [24].

In this paper, we propose a URA scheme over MIMO fading channels, employing pilot transmission for user detection and channel estimation, similar to [26]–[28]. Unlike the previous works that use a single non-orthogonal pilot sequence, in the proposed scheme, each user employs multiple stages of orthogonal pilots selected randomly from a codebook. Since the orthogonality of the pilots in different stages removes the interference, the performance of the pilot detection and channel estimation algorithms in the proposed scheme is improved compared to the decoding performance of the schemes using non-orthogonal pilots. We demonstrate that, while the covariance-based AD algorithm in [24] suffers from high computational complexity in large blocklengths, and the algorithms in [25], [26] do not work well in the short blocklength regime (hence not suitable for fast fading scenarios), the newly proposed algorithm has a superior performance in both short and large blocklength regimes.

The paper is organized as follows. Section II presents the system model for the proposed framework. The encoding and decoding schemes are introduced in Section III. In Section IV, various numerical results are given. Finally, Section V provides our conclusions.

The following notation is adopted throughout the paper. We denote the set of imaginary numbers by \mathbb{C} . $[\mathbf{T}]_{(l,:)}$ and $[\mathbf{T}]_{(:,l)}$ are the l th row and the l th column of \mathbf{T} , respectively. $\text{Re}(\mathbf{t})$ and $\text{Im}(\mathbf{t})$ are used for the real and imaginary parts of \mathbf{t} ; and, the transpose and Hermitian of matrix \mathbf{T} are denoted by \mathbf{T}^T and \mathbf{T}^H , respectively. The notation $|\cdot|$ is used for the

cardinality of a set, and \mathbf{I}_M denotes an $M \times M$ identity matrix.

II. SYSTEM MODEL

We consider an unsourced random access model over a block-fading wireless channel. The BS is equipped with M receiving antennas connected to K_T potential users, for which K_a of them are active in a given frame. Assuming that the channel coherence time is larger than L , we divide the length- n time-frame into S slots of length L ($n = SL$). Each active user randomly selects a single slot to transmit B bits of information. In the absence of synchronization errors, the received signal vector corresponding to the l th slot at the m th antenna is written as

$$\mathbf{y}_{m,l} = \sum_{i \in \mathcal{K}_l} h_{m,i} \mathbf{x}(\mathbf{w}(i)) + \mathbf{z}_{m,l}, \quad (1)$$

where $\mathbf{y}_{m,l} \in \mathbb{C}^{1 \times L}$, \mathcal{K}_l denotes the set of active user indices available in the l th slot, $\mathbf{x}(\mathbf{w}(i)) \in \mathbb{C}^{1 \times L}$ is the encoded and modulated signal corresponding to the message bit sequence $\mathbf{w}(i) \in \{0,1\}^B$ of user i , $h_{m,i} \sim \mathcal{CN}(0,1)$ is the Rayleigh channel coefficient between the i th user and the m th receive antenna, and $\mathbf{z}_{m,l} \sim \mathcal{CN}(\mathbf{0}, \mathbf{I}_L)$ is the circularly symmetric complex white Gaussian noise vector. Letting \mathcal{K}_a and \mathcal{L}_d denote the set of active user indices and the list of decoded messages, respectively, the PUPE of the system is defined in terms of the probability of false-alarm, p_{fa} , and the probability of missed-detection, p_{md} , as

$$P_e = p_{fa} + p_{md}, \quad (2)$$

where

$$p_{md} = \frac{1}{K_a} \sum_{i \in \mathcal{K}_a} \Pr(\mathbf{w}(i) \notin \mathcal{L}_d), \quad p_{fa} = \mathbb{E} \left\{ \frac{n_{fa}}{|\mathcal{L}_d|} \right\}, \quad (3)$$

with n_{fa} being the number of decoded messages that were indeed not sent. The energy-per-bit of the system can be written as $E_b/N_0 = LP/B$, where P denotes the average power of each user per channel use. The objective is to minimize the required energy-per-bit for a target PUPE.

III. THE PROPOSED SCHEME

A. Encoder

As shown in Fig. 1, we divide the message of the i th user into $J + 1$ parts (one data part and J pilot parts) denoted by $\mathbf{w}_c(i)$ and $\mathbf{w}_{p_j}(i)$, $j = 1, 2, \dots, J$ with lengths B_c and B_p , respectively, where $B_c + JB_p = B$. The i th user obtains its j th pilot sequence, \mathbf{b}_{ji} , with length $n_p = 2^{B_p}$ by mapping $\mathbf{w}_{p_j}(i)$ to the orthogonal rows of an $n_p \times n_p$ Hadamard matrix \mathbf{B}_{n_p} , which is generated as

$$\mathbf{B}_2 = \begin{bmatrix} 1 & 1 \\ 1 & -1 \end{bmatrix}, \quad \mathbf{B}_{2^i} = \mathbf{B}_2 \otimes \mathbf{B}_{2^{i-1}} \quad \forall i = 2, 3, \dots,$$

where \otimes represents the Kronecker product. Since the number of possible pilots in the orthogonal Hadamard codebook is limited, it is likely that the users are in collision in certain pilot segments, that is, they share the same pilots with the other users. However, it is highly unlikely that a given user will

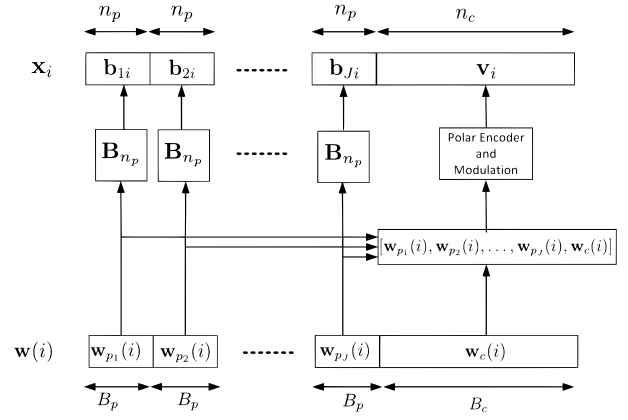


Fig. 1. Illustration of the encoding process in the proposed unsourced scheme.

experience collision in all the pilot segments. To construct the coded sequence of the i th user, we accumulate all the message parts in a row vector as

$$\mathbf{w}(i) = [\mathbf{w}_{p_1}(i), \mathbf{w}_{p_2}(i), \dots, \mathbf{w}_{p_J}(i), \mathbf{w}_c(i)], \quad (4)$$

and pass it to a $(2n_c, B + r)$ polar code, where r is the number of cyclic redundancy check (CRC) bits. Note that contrary to the existing schemes in URA, we feed not only the data bits but also the pilot bit sequences to the encoder. Hence, in the case of successful decoding, all the pilot sequences for the user can be retrieved. The polar codeword is then modulated using quadrature phase shift keying (QPSK), resulting in $\mathbf{v}_i \in \{\sqrt{P_c/2}(\pm 1 \pm j)\}^{1 \times n_c}$, where P_c is the average power of the polar coded part. The transmitted signal for the i th user also consists of J pilot parts and one coded part as

$$\mathbf{x}_i = [\sqrt{P_p} \mathbf{b}_{1i}, \sqrt{P_p} \mathbf{b}_{2i}, \dots, \sqrt{P_p} \mathbf{b}_{Ji}, \mathbf{v}_i] \in \mathbb{C}^{1 \times L} \quad (5)$$

where $\mathbf{x}_i := \mathbf{x}(\mathbf{w}(i))$, $L = n_c + Jn_p$, and P_p denotes the average power of the pilot sequence.

The j th pilot part and the polar coded part of the received signal in the l th slot can be modeled as

$$\mathbf{Y}_{p_j} = \sqrt{P_p} \mathbf{H} \mathbf{B}_j + \mathbf{Z}_{p_j} \in \mathbb{C}^{M \times n_p}, \quad j = 1, 2, \dots, J, \quad (6)$$

$$\mathbf{Y}_c = \mathbf{H} \mathbf{V} + \mathbf{Z}_c \in \mathbb{C}^{M \times n_c}, \quad (7)$$

where $\mathbf{H} \in \mathbb{C}^{M \times K_l}$ is the channel coefficient matrix with $h_{m,i}$ in its m th row and i th column, K_l is the number of users in the l th slot, \mathbf{Z}_{p_j} and \mathbf{Z}_c consist of independent and identically distributed (i.i.d.) noise samples drawn from $\mathcal{CN}(0,1)$ (i.e., a circularly symmetric complex Gaussian distribution), and the i th rows of $\mathbf{B}_j \in \{\pm 1\}^{K_l \times n_p}$ and $\mathbf{V} \in \{\sqrt{P_c/2}(\pm 1 \pm j)\}^{K_l \times n_c}$ are \mathbf{b}_{ji} and \mathbf{v}_i , respectively. Note that we have removed the slot indices from the above matrices to simplify the notation.

B. Decoder

Decoding in each slot is performed using an iterative process. At each iteration, we decode the transmitted codewords

by employing one of the J pilot parts (sequentially) and the coded part of the received signal in (6) and (7). Generally, only the non-colliding users can be decoded. Some non-colliding users in the current pilot stage may experience collision in the other pilot transmission parts. Therefore, by successfully decoding and removing them using successive interference cancellation (SIC), the collision density is reduced in the other pilot parts. Repeating the decoding iterations, the effects of such collisions are ameliorated.

The decoding process is comprised of five different steps that work in tandem. A pilot detector based on a Neyman-Pearson (NP) test identifies the active pilots in the current pilot part; channel coefficients corresponding to the detected pilots are estimated using a channel estimator; a maximum-ratio combining (MRC) estimator is used to produce a soft estimate of the modulated signal; after demodulation, the signal is passed to a polar list decoder; and, the resulting sequences satisfying the CRC are added to the list of successfully decoded signals before being subtracted from the received signal via SIC. The process is repeated until there are no successfully decoded users in J consecutive SIC iterations. In the following, \mathbf{Y}'_{p_j} and \mathbf{Y}'_c denote the received signals in (6) and (7) after removing the list of messages successfully decoded in the current slot up to the current iteration.

1) *Pilot Detection Based on NP Hypothesis Testing*: At the j th pilot part, we can write the following binary hypothesis testing problem:

$$\begin{aligned} \mathbf{u}_{ji} | \mathcal{H}_0 &\sim \mathcal{CN}(\mathbf{0}, \mathbf{I}_M) \\ \mathbf{u}_{ji} | \mathcal{H}_1 &\sim \mathcal{CN}(\mathbf{0}, \sigma_1^2 \mathbf{I}_M), \end{aligned} \quad (8)$$

where $\sigma_1 = \sqrt{1 + m_{ij} n_p P_p}$, $\mathbf{u}_{ji} = \mathbf{Y}'_{p_j} \bar{\mathbf{b}}_i^H / \sqrt{n_p}$, with $\bar{\mathbf{b}}_i = [\mathbf{B}_{n_p}]_{(i,:)}$, \mathcal{H}_1 and \mathcal{H}_0 are alternative and null hypotheses that show the existence and absence of the pilot $\bar{\mathbf{b}}_i$ at the j th pilot part, respectively, and m_{ij} is the number of users that pick the pilot $\bar{\mathbf{b}}_i$ as their j th pilots. Let $\hat{\mathcal{D}}_j$ be the estimate of the set of active rows of \mathbf{B}_{n_p} in the j th pilot part. Using a γ -level Neyman-Pearson hypothesis testing (where γ is the bound on the false-alarm probability), $\hat{\mathcal{D}}_j$ can be obtained as (see Appendix A for details)

$$\hat{\mathcal{D}}_j = \left\{ l : \mathbf{u}_{jl}^H \mathbf{u}_{jl} \geq \frac{1}{2} \Gamma_{2M}^{-1}(1 - \gamma) \right\}, \quad (9)$$

where $\Gamma_k(\cdot)$ denotes the cumulative distribution function of the chi-squared distribution with k degrees of freedom, and $\Gamma_k^{-1}(\cdot)$ is its inverse. The probability of detection in the absence of collision ($m_{ij} = 1$) is obtained in (25). Note that a higher probability of detection is obtained in the general case of $m_{ij} > 1$. It is clear that the probability of detection is controlled by the parameters γ , n_p , and P_p .

2) *Channel Estimation*: Let $\mathbf{B}_{\hat{\mathcal{D}}_j} \in \{\pm 1\}^{|\hat{\mathcal{D}}_j| \times n_p}$ be a sub-matrix of \mathbf{B}_{n_p} consisting of the detected pilots in (9), and suppose that $\tilde{\mathbf{b}}_{jk} = [\mathbf{B}_{\hat{\mathcal{D}}_j}]_{(k,:)}$ is the corresponding pilot of the i th user. Since the rows of the codebook are orthogonal to each other, the channel coefficient vector of the i th user can

be estimated as

$$\hat{\mathbf{h}}_i = \frac{1}{n_p \sqrt{P_p}} \mathbf{Y}'_{p_j} \tilde{\mathbf{b}}_{jk}^H. \quad (10)$$

Note that if the i th user is in a collision (i.e., more than one user selects $\tilde{\mathbf{b}}_{jk}$), Eq. 10 gives an unreliable estimate of the channel coefficient vector. However, this is unimportant since a CRC check is employed after decoding and such errors do not propagate.

3) *MRC, Demodulation, and Channel Decoding*: Let \mathbf{h}_i be the channel coefficient vector of the i th user, where $i \in \tilde{\mathcal{S}}_l$ with $\tilde{\mathcal{S}}_l$ denoting the set of remaining messages in the l th slot. Using $\hat{\mathbf{h}}_i$ in (10), the modulated signal of the i th user can be estimated employing the MRC technique as

$$\hat{\mathbf{v}}_i = \hat{\mathbf{h}}_i^H \mathbf{Y}'_c. \quad (11)$$

Plugging (7) into (11), $\hat{\mathbf{v}}_i$ is written as

$$\hat{\mathbf{v}}_i = \hat{\mathbf{h}}_i^H \mathbf{h}_i \mathbf{v}_i + \sum_{k \in \tilde{\mathcal{S}}_l, k \neq i} \hat{\mathbf{h}}_i^H \mathbf{h}_k \mathbf{v}_k + \hat{\mathbf{h}}_i^H \mathbf{Z}_c. \quad (12)$$

The first term in (12) is the signal term, and the second and third terms are the interference and noise terms, respectively. Since $E\{\mathbf{v}_k^H \mathbf{v}_k\} = P_c \mathbf{I}_{n_c}$, the power of each term can be calculated as

$$\hat{\sigma}_{si}^2 \approx P_c \|\hat{\mathbf{h}}_i\|^4, \quad (13)$$

$$\hat{\sigma}_{Ii}^2 = P_c \sum_{k \in \tilde{\mathcal{S}}_l, k \neq i} |\hat{\mathbf{h}}_i^H \mathbf{h}_k|^2 \approx P_c \sum_{k \in \hat{\mathcal{D}}_j, k \neq i} |\hat{\mathbf{h}}_i^H \hat{\mathbf{h}}_k|^2, \quad (14)$$

$$\hat{\sigma}_{ni}^2 = \|\hat{\mathbf{h}}_i\|^2. \quad (15)$$

Assuming that the interference-plus-noise in (12) is approximately Gaussian-distributed, the following log-likelihood ratio (LLR) is obtained as the input to the polar list decoder

$$\mathbf{f}_i = [\text{Im}(\beta_{1i}), \text{Re}(\beta_{1i}), \dots, \text{Im}(\beta_{n_c i}), \text{Re}(\beta_{n_c i})], \quad (16)$$

$$\beta_{ti} = \frac{2\sqrt{\hat{\sigma}_{si}^2}}{\hat{\sigma}_{ni}^2 + \hat{\sigma}_{Ii}^2} [\hat{\mathbf{v}}_i]_{(:,t)}. \quad (17)$$

At the j th pilot part, the i th user is declared as successfully decoded if 1) its decoded message satisfies the CRC check, and 2) by mapping the j th pilot part of its decoded message to the Hadamard codebook, \mathbf{b}_{jk} is obtained. Then, all the successfully decoded messages (in the current and previous iterations) are accumulated in the set \mathcal{S}_l , where $|\mathcal{S}_l| + |\tilde{\mathcal{S}}_l| = K_l$.

4) *SIC*: we can see in (4) that the successfully decoded messages contain bit sequences of pilot parts and the coded part ($\mathbf{w}_{p_j(i)}$, $j = 1, 2, \dots, J$ and $\mathbf{w}_c(i)$). Having the bit sequences of successfully decoded messages, we can construct the corresponding transmitted signals using (5). The received signal matrix can be written as

$$\mathbf{Y} = \mathbf{H}_{\mathcal{S}_l} \mathbf{X}_{\mathcal{S}_l} + \mathbf{H}_{\tilde{\mathcal{S}}_l} \mathbf{X}_{\tilde{\mathcal{S}}_l} + \mathbf{Z}_l, \quad (18)$$

where \mathbf{Y} is obtained by merging received signal matrices of different parts, i.e., $\mathbf{Y} = [\mathbf{Y}_{p_1}, \dots, \mathbf{Y}_{p_J}, \mathbf{Y}_c] \in \mathbb{C}^{M \times L}$ with $\mathbf{X}_{\mathcal{S}_l} \in \mathbb{C}^{|\mathcal{S}_l| \times L}$ and $\mathbf{X}_{\tilde{\mathcal{S}}_l} \in \mathbb{C}^{|\tilde{\mathcal{S}}_l| \times L}$ being constructed using

the signals in the sets \mathcal{S}_l and $\tilde{\mathcal{S}}_l$, and $\mathbf{H}_{\mathcal{S}_l} \in \mathbb{C}^{M \times |\mathcal{S}_l|}$ and $\mathbf{H}_{\tilde{\mathcal{S}}_l} \in \mathbb{C}^{M \times |\tilde{\mathcal{S}}_l|}$ comprise the channel coefficients corresponding to users in the sets \mathcal{S}_l and $\tilde{\mathcal{S}}_l$, respectively. Considering $\mathbf{H}_{\tilde{\mathcal{S}}_l} \mathbf{X}_{\tilde{\mathcal{S}}_l} + \mathbf{Z}_l$ as an additive noise term, $\mathbf{H}_{\mathcal{S}_l}$ can be estimated by applying the least squares (LS) estimation on (18) as

$$\hat{\mathbf{H}}_{\mathcal{S}_l} = \mathbf{Y} \mathbf{X}_{\mathcal{S}_l}^H (\mathbf{X}_{\mathcal{S}_l} \mathbf{X}_{\mathcal{S}_l}^H)^{-1}. \quad (19)$$

Note that $\mathbf{X}_{\mathcal{S}_l}$ consists of all the successfully decoded signals so far in the l th slot, and \mathbf{Y} is the initially received signal matrix, not the output of the latest SIC iteration. The SIC procedure is performed as follows

$$\mathbf{Y}' = [\mathbf{Y}'_{p_1}, \mathbf{Y}'_{p_2}, \dots, \mathbf{Y}'_{p_J}, \mathbf{Y}'_c] = \mathbf{Y} - \hat{\mathbf{H}}_{\mathcal{S}_l} \mathbf{X}_{\mathcal{S}_l}. \quad (20)$$

Finally, \mathbf{Y}' is fed back to the pilot detection algorithm for the next SIC iteration. The details of decoding stages are shown in Fig. 2 and Algorithm 1.

Algorithm 1: The proposed decoding scheme.

```

for  $l = 0, 1, \dots, S$  do Different slots
   $\mathcal{S}_l = \emptyset$ .
  flag = 1.
   $t = 0$  ( $t$  shows iteration index).
  while flag = 1 do
     $t = t + 1$ .
    for  $j = 1, 2, \dots, J$  do different pilot parts
      Pilot detection: estimate  $\hat{\mathcal{D}}_j$  using (9).
      for  $i \in \hat{\mathcal{D}}_j$  do different detected pilots
        Ch. estimation: estimate  $\hat{\mathbf{h}}_i$  using (10).
        Decoding: pass  $\mathbf{f}_i$  in (16) to list decoder.
         $\mathcal{S}_{tj}$ : set of successfully decoded users in the
          current iteration.
         $\mathcal{S}_l = \mathcal{S}_l \cup \mathcal{S}_{tj}$ .
        SIC: update  $\mathbf{Y}'_{p_j}$  and  $\mathbf{Y}'_c$  using (20).
      end
    end
    if  $\bigcup_{j=1}^J \mathcal{S}_{tj} = \emptyset$  then
      flag = 0.
    end
  end
end
end

```

IV. NUMERICAL RESULTS

In this section, we provide a set of numerical results to assess the performance of the proposed URA scheme. In all the results, we set the list size of the decoder to 64, $B = 100$, the frame length $n \cong 3200$, the number of CRC bits $r = 11$, the Neyman-Pearson threshold $\gamma = 0.001$, and $P_e = 0.05$.

In Fig. 3, the performance of the proposed scheme is compared with the short blocklength scheme of [24] with the number of antennas $M = 100$ and slot lengths $L = 320$ and 200. For a fair comparison, we consider two scenarios with $(J, n_p, n_c) = (2, 32, 256)$ (corresponding to $L = 320$) and $P_c/P_p = 0.5$, and $(J, n_p, n_c) = (2, 32, 128)$ ($L = 192$) and $P_c/P_p = 1$, respectively. It is illustrated in this figure that the proposed decoder significantly outperforms the approach in [24].

To compare the proposed framework with the ones in [25]

and [26], we set $(J, n_p, n_c) = (2, 256, 512)$, $M = 50$, $P_c/P_p = 1.5$, and depict the results in Fig. 4. It is clear that the proposed solution has a superior performance for this increased blocklength as well. We note that the blocklength employed in the proposed algorithm is 3 times shorter than those used in [25], [26]. Using a larger blocklength would improve the system performance at the cost of higher computational complexity. To show the effect of the parameter n_p on the performance of the proposed scheme, we provide several examples for $n_c = 512$, $J = 2$, $M = 50$, $P_c/P_p = 1.5$ in Fig. 5. It is observed that the performance of the decoder is highly sensitive to this parameter, especially, for larger values of K_a .

In Fig. 6, the performance of the Neyman-Pearson detector is shown for two different values of n_p and M . It is demonstrated that if we select the value of P_p greater than 0.005 and 0.02, the probability of detection is around 1. Since the values of P_p selected for reaching the target PUPE in Figs. 3 and 4 are greater than these values, we benefit from the excellent pilot detection performance in these scenarios. It is also evident from these results that the detection probabilities obtained by simulations match the analytical result in (25).

Finally, we note that a new scheme called FASURA has been reported in [29] after the submission of this paper. In FASURA, each user transmits a large blocklength signal containing a non-orthogonal pilot and a randomly spread polar code. FASURA offers improved performance for large blocklengths while our scheme remains superior for short blocklengths.

V. CONCLUSIONS

We propose an unsourced MAC scheme for block fading channels using a massive MIMO structure. The proposed scheme uses multiple stages of orthogonal pilots for pilot detection and channel estimation. The use of small-length orthogonal multi-stage pilots makes the system implementable for short blocklength scenarios. The results demonstrate that the proposed approach is superior to the existing alternatives developed in the recent literature.

APPENDIX A

PERFORMANCE OF THE NP HYPOTHESIS TESTING

The likelihood ratio for (8) is given by

$$L(\mathbf{u}_{ji}) = \frac{\mathbb{P}(\mathbf{u}_{ji} | \mathcal{H}_1)}{\mathbb{P}(\mathbf{u}_{ji} | \mathcal{H}_0)} = \frac{1}{\sigma_1^M} e^{\mathbf{u}_{ji}^H \mathbf{u}_{ji} / \sigma_0^2}, \quad (21)$$

where $\sigma_0^2 = \frac{2(1 + m_{ij} n_p P_p)}{m_{ij} n_p P_p}$. Thus, the Neyman-Pearson test for detection of $\bar{\mathbf{b}}_i$ is obtained by

$$\delta_{NP}(\mathbf{u}_{ji}) = \begin{cases} 1 & L(\mathbf{u}_{ji}) \geq \tau_0 \\ 0 & L(\mathbf{u}_{ji}) < \tau_0 \end{cases} = \begin{cases} 1 & \mathbf{u}_{ji}^H \mathbf{u}_{ji} \geq \tau'_0 \\ 0 & \mathbf{u}_{ji}^H \mathbf{u}_{ji} < \tau'_0 \end{cases}, \quad (22)$$

where $\tau'_0 = \sigma_0^2 \text{Ln}(\tau_0 \sigma_1^M)$. The false-alarm probability of the above decision rule is calculated as

$$P_F(\delta_{NP}) = \mathbb{P}(\mathbf{u}_{ji}^H \mathbf{u}_{ji} \geq \tau'_0 | \mathcal{H}_0) \stackrel{(a)}{=} 1 - \Gamma_{2M}(2\tau'_0), \quad (23)$$

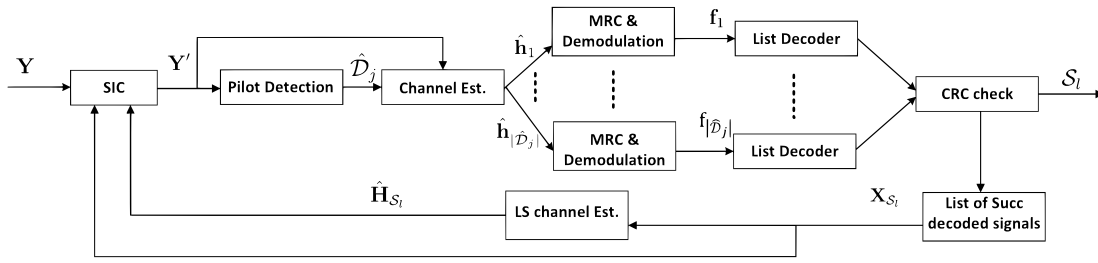


Fig. 2. The decoding process at the j th pilot part and the l th slot.

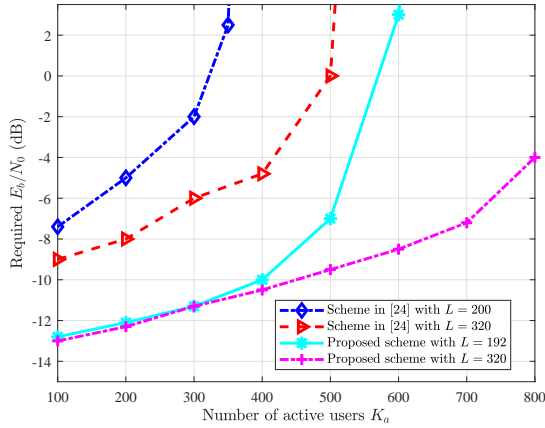


Fig. 3. The required E_b/N_0 as a function of the number of active users in the proposed scheme and the method in [24] for $M = 100$ and $L \approx 320, 200$.

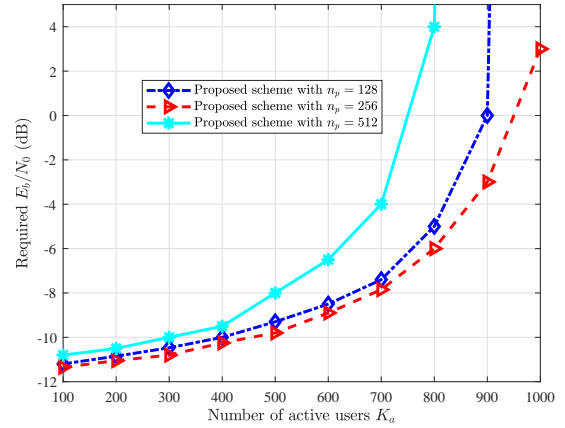


Fig. 5. The required E_b/N_0 as a function of the number of active users in the proposed scheme for $M = 50$, $J = 2$, and different values of n_p .

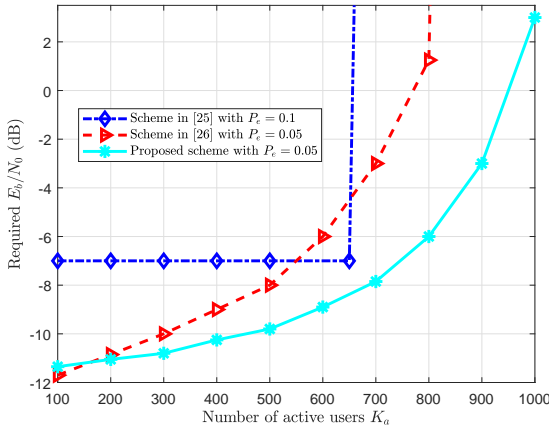


Fig. 4. The required E_b/N_0 as a function of the number of active users in the proposed scheme and the results in [25], [26] for $M = 50$.

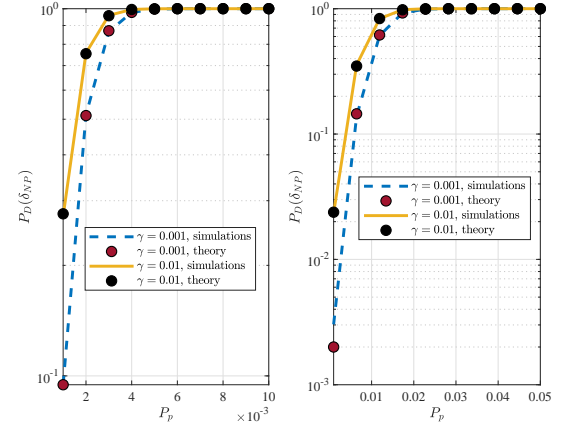


Fig. 6. Comparison of the simulation and analytical performance of the pilot detector for $M = 50$ and $n_p = 256$ (left), and $M = 100$ and $n_p = 32$ (right).

where (a) follows the fact that $\mathbf{u}_{ji}^H \mathbf{u}_{ji} | \mathcal{H}_0 \sim 0.5\chi_{2M}^2$ and $\mathbf{u}_{ji}^H \mathbf{u}_{ji} | \mathcal{H}_1 \sim 0.5\sigma_1^2 \chi_{2M}^2$, and χ_k^2 denotes the chi-squared distribution with k degrees of freedom. To find the threshold for a γ -level Neyman-Pearson test, the probability of the false-alarm in (23) must satisfy $P_F(\delta_{NP}) \leq \gamma$. Therefore, the threshold in (22) is obtained as

$$\tau'_0 = \frac{1}{2} \Gamma_{2M}^{-1}(1 - \gamma). \quad (24)$$

The probability of detection in the absence of collision ($m_{ij} = 1$) is then obtained as

$$\begin{aligned} P_D(\delta_{NP}) &= \mathbb{P}(\mathbf{u}_{ji}^H \mathbf{u}_{ji} \geq \tau'_0 | \mathcal{H}_1) \\ &= 1 - \Gamma_{2M} \left(\frac{2\tau'_0}{1 + n_p P_p} \right) \\ &= 1 - \Gamma_{2M} \left(\frac{\Gamma_{2M}^{-1}(1 - \gamma)}{1 + n_p P_p} \right). \end{aligned} \quad (25)$$

REFERENCES

- [1] T. L. Marzetta, "Noncooperative cellular wireless with unlimited numbers of base station antennas," *IEEE Trans. Wireless Commun.*, vol. 9, no. 11, pp. 3590–3600, Nov. 2010.
- [2] E. Björnson, E. G. Larsson and M. Debbah, "Massive MIMO for maximal spectral efficiency: how many users and pilots should be allocated?," *IEEE Trans. Wireless Commun.*, vol. 15, no. 2, pp. 1293–1308, Feb. 2016.
- [3] E. Björnson, J. Hoydis, and L. Sanguinetti, "Massive MIMO networks: spectral, energy, and hardware efficiency," *Found. Trends Signal Process.*, vol. 11, no. 3-4, pp. 154–655, Nov. 2017.
- [4] J. Hoydis, S. ten Brink and M. Debbah, "Massive MIMO in the UL/DL of cellular networks: how many antennas do we need?," *IEEE J. Sel. Areas Commun.*, vol. 31, no. 2, pp. 160–171, Feb. 2013.
- [5] Y. Polyanskiy, "A perspective on massive random-access," in *Proc. IEEE Int. Symp. Inf. Theory (ISIT)*, Aachen, Germany, June 2017, pp. 2523–2527.
- [6] O. Ordentlich and Y. Polyanskiy, "Low complexity schemes for the random access Gaussian channel," in *Proc. IEEE Int. Symp. Inf. Theory (ISIT)*, Aachen, Germany, June 2017, pp. 2528–2532.
- [7] G. Kasper Facenda and D. Silva, "Efficient scheduling for the massive random access Gaussian channel," *IEEE Trans. Wireless Commun.*, vol. 19, no. 11, pp. 7598–7609, Nov. 2020.
- [8] A. Vem, K. R. Narayanan, J.-F. Chamberland, and J. Cheng, "A user-independent successive interference cancellation based coding scheme for the unsourced random access Gaussian channel," *IEEE Trans. Commun.*, vol. 67, no. 12, pp. 8258–8272, Dec. 2019.
- [9] A. Glebov, N. Matveev, K. Andreev, A. Frolov and A. Turlikov, "Achievability bounds for T-fold irregular repetition slotted ALOHA scheme in the Gaussian MAC," in *Proc. IEEE Wireless Commun. Netw. Conf. (WCNC)*, Marrakesh, Morocco, Apr. 2019, pp. 1–6.
- [10] V. K. Amalladinne, A. Vem, D. K. Soma, K. R. Narayanan, and J.-F. Chamberland, "A coupled compressive sensing scheme for unsourced multiple access," in *Proc. IEEE Int. Conf. Acoust., Speech Signal Process. (ICASSP)*, Calgary, Canada, Sep. 2018, pp. 6628–6632.
- [11] M. Zheng, Y. Wu, and W. Zhang, "Polar coding and sparse spreading for massive unsourced random access," in *Proc. IEEE Veh. Technol. Conf. (VTC)*, Victoria, Canada, Feb. 2020, pp. 1–5.
- [12] A. K. Tanc and T. M. Duman, "Massive random access with trellis based codes and random signatures," *IEEE Commun. Lett.*, vol. 25, no. 5, pp. 1496–1499, May 2021.
- [13] Z. Han, X. Yuan, C. Xu, S. Jiang and X. Wang, "Sparse Kronecker-product coding for unsourced multiple access," *IEEE Wireless Commun. Lett.*, vol. 10, no. 10, pp. 2274–2278, Oct. 2021.
- [14] J. R. Ebert, V. K. Amalladinne, S. Rini, J. -F. Chamberland and K. R. Narayanan, "Stochastic binning and coded demixing for unsourced random access," in *Proc. IEEE Workshop Signal Process. Adv. Wireless Commun. (SPAWC)*, Lucca, Italy, Sep. 2021, pp. 351–355.
- [15] A. K. Pradhan, V. K. Amalladinne, K. R. Narayanan, and J.-F. Chamberland, "Polar coding and random spreading for unsourced multiple access," in *Proc. IEEE Int. Conf. Commun. (ICC)*, Dublin, Ireland, June 2020, pp. 1–6.
- [16] M. J. Ahmadi and T. M. Duman, "Random spreading for unsourced MAC with power diversity," in *IEEE Commun. Lett.*, vol. 25, no. 12, pp. 3995–3999, Dec. 2021.
- [17] A. K. Pradhan, V. K. Amalladinne, K. R. Narayanan and J. -F. Chamberland, "LDPC codes with soft interference cancellation for uncoordinated unsourced multiple access," in *Proc. IEEE Int. Conf. Commun. (ICC)*, Montreal, Canada, June 2021, pp. 1–6.
- [18] S. S. Kowshik and Y. Polyanskiy, "Quasi-static fading MAC with many users and finite payload," in *Proc. IEEE Int. Symp. Inf. Theory (ISIT)*, Paris, France, July 2019, pp. 440–444.
- [19] S. S. Kowshik, K. Andreev, A. Frolov and Y. Polyanskiy, "Energy efficient coded random access for the wireless uplink," *IEEE Trans. Commun.*, vol. 68, no. 8, pp. 4694–4708, Aug. 2020.
- [20] S. S. Kowshik, K. Andreev, A. Frolov and Y. Polyanskiy, "Energy efficient random access for the quasi-static fading MAC," in *Proc. IEEE Int. Symp. Inf. Theory (ISIT)*, Paris, France, July 2019, pp. 2768–2772.
- [21] S. S. Kowshik and Y. Polyanskiy, "Fundamental limits of many-user MAC with finite payloads and fading," *IEEE Trans. Inf. Theory*, vol. 67, no. 9, pp. 5853–5884, Sep. 2021.
- [22] K. Andreev, S. S. Kowshik, A. Frolov and Y. Polyanskiy, "Low complexity energy efficient random access scheme for the asynchronous fading MAC," in *Proc. IEEE Veh. Technol. Conf. (VTC)*, Honolulu, USA, Sep. 2019, pp. 1–5.
- [23] V. K. Amalladinne, K. R. Narayanan, J. -F. Chamberland and D. Guo, "Asynchronous neighbor discovery using coupled compressive sensing," in *Proc. IEEE Int. Conf. Acoust., Speech Signal Process. (ICASSP)*, Brighton, UK, May 2019, pp. 4569–4573.
- [24] A. Fengler, S. Haghghatshoar, P. Jung and G. Caire, "Non-Bayesian activity detection, large-scale fading coefficient estimation, and unsourced random access with a massive MIMO receiver," *IEEE Trans. Inf. Theory*, vol. 67, no. 5, pp. 2925–2951, May 2021.
- [25] A. Decurninge, I. Land and M. Guillaud, "Tensor-based modulation for unsourced massive random access," *IEEE Wireless Commun. Lett.*, vol. 10, no. 3, pp. 552–556, Mar. 2021.
- [26] A. Fengler, P. Jung and G. Caire, "Pilot-based unsourced random access with a massive MIMO receiver in the Quasi-static fading regime," in *Proc. IEEE Workshop Signal Process. Adv. Wireless Commun. (SPAWC)*, Lucca, Italy, Sep. 2021, pp. 356–360.
- [27] L. Liu and W. Yu, "Massive connectivity with massive MIMO—Part I: device activity detection and channel estimation," in *IEEE Trans. Signal Process.*, vol. 66, no. 11, pp. 2933–2946, June 2018.
- [28] K. Senel and E. G. Larsson, "Grant-Free massive MTC-Enabled massive MIMO: a compressive sensing approach," *IEEE Trans. Commun.*, vol. 66, no. 12, pp. 6164–6175, Dec. 2018.
- [29] M. Gkagkos, K. R. Narayanan, J. F. Chamberland and C. N. Georghiadis, "FASURA: A scheme for quasi-static massive MIMO unsourced random access channels," arXiv preprint arXiv:2202.11042.